J|A|C|S ARTICLES

Published on Web 11/02/2010

Stopped-Flow Kinetic Analysis of the Interaction of Cyclo[8]pyrrole with Anions

Elizabeth Karnas,[†] Sung Kuk Kim,[†] Kenneth A. Johnson,*[,†] Jonathan L. Sessler,*[,†,‡] Kei Ohkubo,[§] and Shunichi Fukuzumi*[,§,||]

Department of Chemistry & Biochemistry, University Station-A5300, The University of Texas, Austin, Texas 78712-0165, United States, Department of Chemistry, Yonsei University, Seoul 120-749, Korea, Department of Material and Life Science, Graduate School of Engineering, Osaka University, Suita, Osaka 565-0871, Japan, and Department of Bioinspired Science, Ewha Womans University, Seoul 120-750, Korea

Received August 18, 2010; Revised Manuscript Received September 23, 2010; E-mail: kajohnson@mail.utexas.edu; sessler@mail.utexas.edu; fukuzumi@chem.eng.osaka-u.ac.jp

Abstract: The on and off rates corresponding to the binding of two test anions (acetate, AcO^-, and dihydrogen phosphate, $H_2PO_4^-$, studied as their tetrabutylammonium salts) to diprotonated cyclo[8]pyrrole have been determined in CH_3CN using stopped-flow analyses carried out at various temperatures. For dihydrogen phosphate, this afforded the activation enthalpies and entropies associated with both off and on processes. The different dynamic behavior seen for these test anions underscores the utility of kinetic analyses as a possible new tool for the advanced characterization of anion receptors.

Introduction

Anion binding has emerged as an important subdiscipline within the broader field of supramolecular chemistry.[1−4] Considerable work has been devoted to the synthesis of new anion receptors and to the characterization of their complexes at equilibrium.[1−7] Yet, few studies have addressed the problem of anion binding dynamics. To date, some insights into the dynamics of receptor−anion interactions (i.e., on and off rates) have been obtained via the use of NMR exchange techniques.[8,9] However, the accessible time scales are limited, and the nature of the process in question must be inferred.

While not well studied, dynamic considerations touch on a number of issues that are critical to both biological and synthetic anion recognition, including apparent receptor−substrate specificities, especially those observed under conditions of slow receptor−anion exchange, as well as the rates of through-membrane ion transport and the viability of liquid−liquid extraction processes.[10] Both extraction and through-membrane transport are dynamic phenomena, meaning the actual utility of an otherwise promising receptor system is likely to be limited

[†] The University of Texas.
[‡] Yonsei University.
[§] Osaka University.
[||] Ewha Womans University.

(1) *Supramolecular Chemistry of Anions*; Bianchi, A., Bowman-James, K., García-España, E., Eds.; Wiley-VCH: New York, 1997.
(2) (a) Piepenbrock, M.-O. M.; Lloyd, G. O.; Clarke, N.; Steed, J. W. *Chem. Rev.* **2010**, *110*, 1960–2004. (b) Paul, R. L.; Bell, Z. R.; Fleming, J. S.; Jeffery, J. C.; McCleverty, J. A.; Ward, M. D. *Heteroatom Chem.* **2002**, *13*, 567–573.
(3) (a) Hua, Y.; Flood, A. H. *Chem. Soc. Rev.* **2010**, *39*, 1262–1271. (b) Gamez, P.; Mooibroek, T. J.; Teat, S. J.; Reedijk, J. *Acc. Chem. Res.* **2007**, *40*, 435–444. (c) Amendola, V.; Esteban-Gomez, D.; Fabbrizzi, L.; Licchelli, M. *Acc. Chem. Res.* **2006**, *39*, 343–353. (d) Beer, P. D.; Gale, P. A. *Angew. Chem., Int. Ed.* **2001**, *40*, 486–516. (e) Gale, P. D. *Chem. Soc. Rev.* **2010**, *39*, 3746–3771.
(4) (a) Juwarker, H.; Suk, J.-m.; Jeong, K.-S. *Chem. Soc. Rev.* **2009**, *38*, 3316–3325. (b) Chang, K.-J.; Kang, B. N.; Lee, M.-H.; Jeong, K.-S. *J. Am. Chem. Soc.* **2005**, *127*, 12214–12215.
(5) (a) Sessler, J. L.; Davis, J. M. *Acc. Chem. Res.* **2001**, *34*, 989–997. (b) Nielsen, K. A.; Sarova, G. H.; Martín-Gomis, L.; Fernández-Lázaro, F.; Stein, P. C.; Sanguinet, L.; Levillain, E.; Sessler, J. L.; Guldi, D. M.; Sastre-Santos, A.; Jeppesen, J. O. *J. Am. Chem. Soc.* **2008**, *130*, 460–462. (c) Nielsen, K. A.; Cho, W.-S.; Lyskawa, J.; Levillain, E.; Lynch, V. M.; Sessler, J. L.; Jeppesen, J. O. *J. Am. Chem. Soc.* **2006**, *128*, 2444–2451.
(6) (a) Nishiyabu, R.; Palacios, M. A.; Dehaen, W.; Anzenbacher, P., Jr. *J. Am. Chem. Soc.* **2006**, *128*, 11496–11504. (b) Kang, S. K.; Powell, D.; Bowman-James, K. *J. Am. Chem. Soc.* **2005**, *127*, 13478–13479. (c) Kano, K.; Kitagishi, H.; Tamura, S.; Yamada., A. *J. Am. Chem. Soc.* **2004**, *126*, 15202–15210.
(7) (a) Yoon, D.-W.; Gross, D. E.; Lynch, V. M.; Sessler, J. L.; Hay, B. P.; Lee, C.-H. *Angew. Chem., Int. Ed.* **2008**, *47*, 5038–5042. (b) Gross, D. E.; Yoon, D.-W.; Lynch, V. M.; Lee, C.-H.; Sessler, J. L. *J. Inclusion Phenom. Macrocyclic Chem.* **2010**, *66*, 81–85. (c) Hay, B. P. *Chem. Soc. Rev.* **2010**, *39*, 3700–3708.
(8) (a) Shi, X.; Mullaugh, K. M.; Fettinger, J. C.; Jiang, Y.; Hofstadler, S. A.; Davis, J. T. *J. Am. Chem. Soc.* **2003**, *125*, 10830–10841. (b) Yamanaka, M.; Toyoda, N.; Kobayashi, K. *J. Am. Chem. Soc.* **2009**, *131*, 9880–9881. (c) Kvasnica, M.; Purse, B. W. *New J. Chem.* **2010**, *34*, 1097–1099.
(9) For a tutorial review on exchange mechanisms in supramolecular host−guest assemblies, see: Pluth, M. D.; Raymond, K. N. *Chem. Soc. Rev.* **2007**, 161–171. For other examples involving exchange dynamics in supramolecular capsule systems, see: (a) Palmer, L. C.; Rebek, J., Jr. *Org. Biomol. Chem.* **2004**, *2*, 3051–3059. (b) Marquez, C.; Hudgins, R. R.; Nau, W. M. *J. Am. Chem. Soc.* **2004**, *126*, 5806–5816. (c) Nakazawa, J.; Sakae, Y.; Aida, M.; Naruta, Y. *J. Org. Chem.* **2007**, *72*, 9448–9455.
(10) (a) McNally, B. A.; O'Neil, E. J.; Nguyen, A.; Smith, B. D. *J. Am. Chem. Soc.* **2008**, *130*, 17274–17275. (b) Davis, J. T.; Okumola, O.; Quesada, R. *Chem. Soc. Rev.* **2010**, *39*, 3843–3862. (c) Gokel, G.; Barkey, N. *New J. Chem.* **2009**, *33*, 947–963. (d) Fowler, C. J.; Haverlock, T. J.; Moyer, B. A.; Shriver, J. A.; Gross, D. E.; Marquez, M.; Sessler, J. L.; Hossain, M. A.; Bowman-James, K. *J. Am. Chem. Soc.* **2008**, *130*, 14386–14387.

Scheme 1. Model Used To Fit the Kinetic Data Obtained upon Mixing **C8**·2HCl with TBAOAc

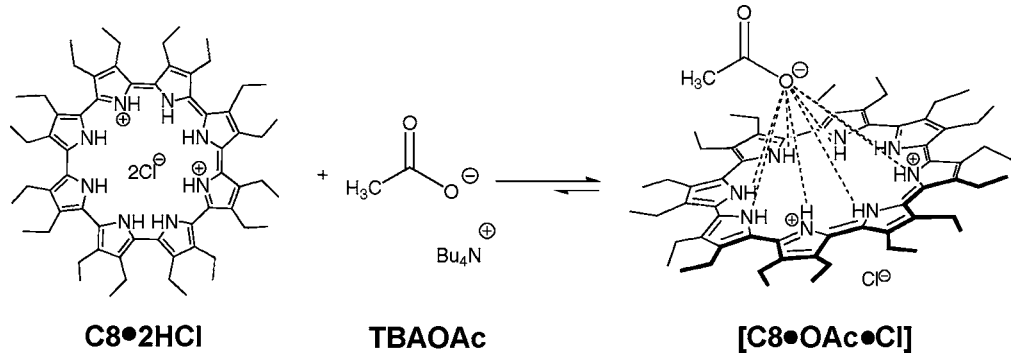

if either ion uptake or release is too slow.[9−11] The same is true for ion-selective electrodes.[12] These potential limitations provide a specific incentive to understand the kinetics of anion recognition.

One approach that might allow the kinetics of anion recognition to be probed in quantitative fashion involves the use of stopped-flow. This technique is frequently used to study the dynamics of enzyme−substrate interactions. It has also recently begun to attract the attention of supramolecular chemists for the analysis of, for example, receptor−cation binding kinetics.[11] However, despite its potential utility, this technique has yet to be extended to the study of anion binding. Here, we report the use of the stopped-flow technique to monitor the on and off rates of two test anions, acetate (AcO^-) and dihydrogen phosphate ($H_2PO_4^-$), binding to diprotonated cyclo[8]pyrrole ([**C8**·2H]$^{2+}$; cf., Scheme 1). To the best of our knowledge, this is the first time the kinetic parameters associated with an anion binding event have been measured in quantitative terms.

Cyclo[8]pyrrole (**C8**), an expanded porphyrin reported by our group in 2002, is able to interact with oxyanions, specifically the sulfate dianion, as was inferred from a single-crystal X-ray diffraction analysis.[13] Follow-up work focused on the application of an organic-solubilized version of **C8** as a possible sulfate extractant. The diprotonated form of this cyclo[8]pyrrole was found to display selectivity for sulfate over nitrate under conditions of aqueous−organic extraction, even in the presence of high concentrations of the latter species.[14] However, this same work also led to the inference that the utility of **C8** as an extractant was limited by the kinetics of anion exchange. More recently, carboxylate and dihydrogen phosphate monoanions were found to bind to **C8** in its diprotonated form ([**C8**·2H]$^{2+}$), as revealed through the significant UV−vis changes upon titration with the corresponding tetrabutylammonium salts. The interactions with carboxylate anions have recently been exploited to create a supramolecular dyad capable of undergoing photoinduced electron transfer.[15] This latter work, based on the use of a pyrene butyric acid salt, prompted the present study. Specifically, we felt it important to characterize the "lifetime" of the supramolecular donor−acceptor, [**C8**·2H]$^{2+}$−carboxylate, complex formed in solution prior to photoexcitation. Understanding the kinetics of association/dissociation is also viewed as being critical to the analysis of other anion-recognition-based ET systems.[16]

In light of this potential benefit, we set out to perform stopped-flow analysis of the interactions between a simple test carboxylate salt, tetrabutylammonium acetate (TBAOAc), and the bis-HCl salt of **C8** (**C8**·2HCl). Because it was found to provide a good spectral signature, an effort was also made to extend this analysis to include the dihydrogen phosphate anion. As detailed below, the present kinetic study also facilitated a determination of the system energetics, including key thermodynamic values, such as enthalpy (ΔH), entropy (ΔS), and free energy change (ΔG). This was accomplished for both anions through van't Hoff analyses made using association constants (K_a) determined at various temperatures through either steady-state measurements, kinetic measurements, or a combination of both. In the case of dihydrogen phosphate, on and off rates could be determined at multiple temperatures. This allowed for an Eyring analysis and yielded the activation parameters ($\Delta H^{\ddagger}$, $\Delta S^{\ddagger}$) for both the on and the off processes. Access to these latter values is limited without quantitative kinetic data.[1]

Results and Discussion

Steady-state titrations were carried out between TBAOAc and **C8**·2HCl in CH_3CN, resulting in large spectral changes in the UV−vis region amenable to study by stopped-flow (Figure 1a). On the basis of a Job plot analysis and curve fits, a 1:1 binding stoichiometry was inferred (Figure 1b). Proton NMR spectroscopic studies provided support for anion binding, as opposed to deprotonation; that is, no loss in the NH proton signal was seen upon treatment with excess anion (see Figure S2).

The apparent association (formally displacement) constant, K_a, for the binding of TBAOAc to **C8**·2HCl in CH_3CN was determined at various temperatures through UV−vis spectral titrations wherein the host concentration is held constant upon

(11) (a) Pace, T. C. S.; Bohne, C. *Adv. Phys. Org. Chem.* **2008**, *42*, 167–223. (b) Bohne, C. *Langmuir* **2006**, *22*, 9100–9111.
(12) Cui, R.; Li, Q.; Gross, D. E.; Meng, X.; Li, B.; Marquez, M.; Yang, R.; Sessler, J. L.; Shao, Y. *J. Am. Chem. Soc.* **2008**, *130*, 14364–14365.
(13) Seidel, D.; Lynch, V.; Sessler, J. L. *Angew. Chem., Int. Ed.* **2002**, *41*, 1422–1425.
(14) Eller, L. R.; Stepien, M.; Fowler, C. J.; Lee, J. T.; Sessler, J. L.; Moyer, B. A. *J. Am. Chem. Soc.* **2007**, *129*, 11020–11021.
(15) Sessler, J. L.; Karnas, E.; Kim, S. K.; Ou, Z.; Zhang, M.; Kadish, K. M.; Ohkubo, K.; Fukuzumi, S. *J. Am. Chem. Soc.* **2008**, *130*, 15256–15257.
(16) (a) D'Souza, F.; Subbaiyan, N. K.; Xie, Y.; Hill, J. P.; Ariga, K.; Ohkubo, K.; Fukuzumi, S. *J. Am. Chem. Soc.* **2009**, *131*, 16138–16146. (b) Springs, S. L.; Gosztola, D.; Wasielewski, M. R.; Kral, V.; Avdrievsky, A.; Sessler, J. L. *J. Am. Chem. Soc.* **1999**, *121*, 2281–2289. (c) Park, J. S.; Karnas, E.; Ohkubo, K.; Chen, P.; Kadish, K. M.; Fukuzumi, S.; Bielawski, C. W.; Hudnall, T. W.; Lynch, V. M.; Sessler, J. L. *Science* **2010**, *329*, 1324–1327. (d) Grimm, B.; Karnas, E.; Brettreich, M.; Ohta, K.; Hirsch, A.; Guldi, D. M.; Torres, T.; Sessler, J. L. *J. Phys. Chem. B* **2009**, *113*, in press. (e) Honda, T.; Nakanishi, T.; Ohkubo, K.; Kojima, T.; Fukuzumi, S. *J. Am. Chem. Soc.* **2010**, *132*, 10155–10163.
(17) **C8**·2HCl was prepared as described in: Köhler, T.; Seidel, D.; Lynch, V.; Arp, F. O.; Ou, Z.; Kadish, K. M.; Sessler, J. L. *J. Am. Chem. Soc.* **2003**, *125*, 6872–6873.

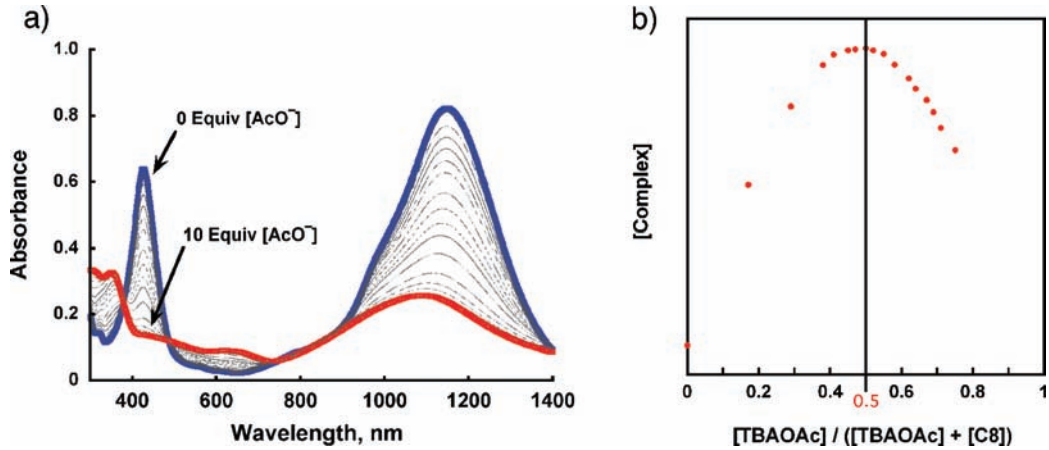

Figure 1. (a) Steady-state spectral titration performed between **C8**·2HCl (1.1×10^{-5} M) and TBAOAc in CH_3CN at 298 K (TBA = tetrabutylammonium). (b) A Job plot was also constructed; it displayed a maxima at a mole fraction of 0.5, as would be expected for a 1:1 binding stoichiometry.

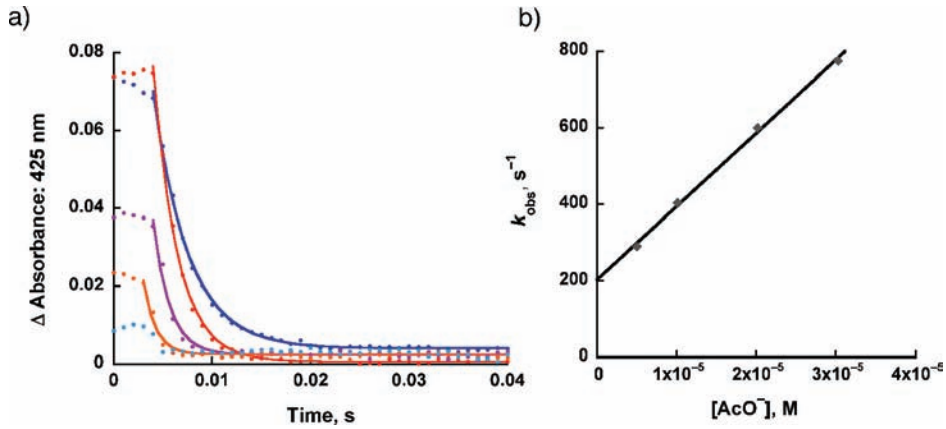

Figure 2. (a) Kinetic traces produced by mixing **C8**·2HCl (4 μM final postmixing concentration) with TBAOAc at the following final concentrations: 5, 10, 20, 30, 50 μM in CH_3CN at 243 K. The mixing time (ca. 3 ms) is shown as dotted lines in these traces. The solid lines represent the fit of a single exponential decay of the signal, giving the observed rate constant, k_{obs}; see text for details. (b) Plot of k_{obs} as a function of the concentration of guest, AcO^-, with a solid line showing the fit to $k_{obs} = k_1[AcO^-] + k_{-1}$, where k_1 is the slope, and k_{-1} is the *y*-intercept.

addition of guest. At 298 K (room temperature), the K_a was found to be on the order of 2×10^5 M^{-1}, and at 243 K, the K_a was found to be on the order of 9×10^4 M^{-1} (see Figure S1). This steady-state data led us postulate that the binding dynamics would be governed by a one-step binding process, as shown in Scheme 1. To test this hypothesis, stopped-flow analyses were carried out in CH_3CN monitoring the change in absorbance from 300−700 nm under conditions of rapid mixing. More specifically, two separate syringes were loaded with stock solutions of the host, **C8**·2HCl, at 8 μM, and the guest, TBAOAc, at various concentrations in CH_3CN. As is typical in a stopped-flow setup, both syringes are automatically and simultaneously engaged to release the same amount (100 μL) of each of the two different solutions into a mixing chamber with a quartz window. This results in a 2-fold dilution of the stock solutions and a rapid mixing. After an initial period in which mixing is presumed to occur (typically 1−3 ms and often referred to as the "dead time"), the flow is stopped, and the optical spectra are recorded as a function of time.[18]

As might be expected given the relatively high K_a value recorded for this anion, the kinetics of interaction with acetate proved to be extremely fast. Indeed, to observe any change in the spectral features of **C8**·2HCl on the ca. millisecond stopped-flow time scale, low temperature (243 K) analyses had to be carried out, and relatively low host concentrations (4 μM) had to be employed. Under these conditions, time-dependent optical changes were observed for a variety of TBAOAc concentrations, as shown in Figure 2 (for the actual time-dependent spectral changes, see Figure S4).

Each kinetic trace obtained could be fit to a single exponential decay as shown in Figure 2. This gave an observed rate constant, k_{obs}, which was then plotted versus the concentration of guest.[18,19] A straight line was obtained, as would be expected for a one-step equilibrium process. By fitting to the equation, $k_{obs} = k_1[AcO^-] + k_{-1}$, the on rate constant ($k_1$) and off rate constant (k_{-1}) could be obtained. This gave values of $k_1 = (1.9 \pm 0.2) \times 10^7$ M^{-1} s^{-1} and k_{-1} of 200 ± 20 s^{-1}, respectively. A value for the K_a, $(9.5 \pm 0.9) \times 10^4$ M^{-1}, was determined from the ratio of k_1/k_{-1}. This kinetically derived association constant proved to be the same within experimental error as that determined by the direct titration discussed above. This concordance, although not a "proof", serves as an important check for the kinetic parameters obtained via stopped flow. The off

(18) *Kinetic Analysis of Macromolecules*; Johnson, K. A., Ed.; Oxford University Press: New York, 2003.

(19) Under the present experimental conditions, the concentration of uncomplexed anion remains approximately constant during the reaction, allowing us to analyze the kinetic data by pseudo-first-order kinetics.

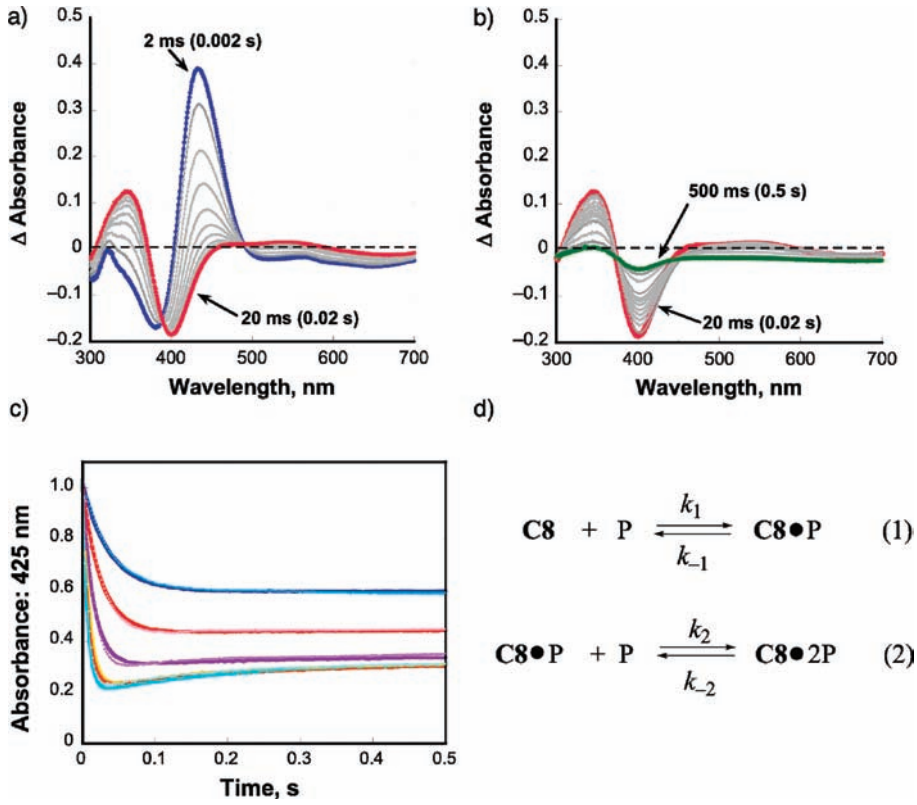

Figure 3. Optical spectra obtained when **C8**·2HCl (10 μM) is mixed under stopped-flow conditions with the 500 μM of $TBAH_2PO_4$ in CH_3CN at 253 K from (a) 2−20 ms and (b) 20−500 ms. (c) Change in the spectral intensity at 425 nm observed when **C8**·2HCl (10 μM) is mixed with 50, 100, 200, 400, 500 μM of $TBAH_2PO_4$ in CH_3CN at 253 K (all concentrations are final, postmixing). The dotted lines are experimental data points corresponding to the decay in the **C8** absorbance at 425 nm, while the solid lines are the best fits obtained using a global fitting procedure.[24] (d) Equations used for the global fitting analysis shown in part (c), wherein "P" represents $H_2PO_4^-$.

rate of 200 s^{-1} corresponds to a lifetime, τ, of 5 ms; this is long enough to allow intraensemble charge separation and recombination as assumed in the previous electron transfer study.[15]

We next analyzed the binding of dihydrogen phosphate ($TBAH_2PO_4$) to **C8**·2HCl. This tetrahedral anion, in contrast to simple carboxylates, is known to form 2:1 complexes with protonated expanded porphyrins, although 1:1 complexes dominate under most solution phase conditions.[20−22] This complexity made $H_2PO_4^-$ useful as a test anion. The raw spectra obtained upon stopped-flow mixing at 253 K are shown in Figure 3.[23] These data provide support for the conclusion that there are at least two steps: a fast phase (Figure 3a) and a slow phase (Figure 3b). It was thus inferred that a reasonable analysis would involve a two-step binding model. Our proposed mechanism involves the binding of first one, and then a second $H_2PO_4^-$ (P), as shown in eqs 1 and 2 (Figure 3d).

Using a global fitting analysis for a two-step process, a k_1 of $(2.65 \pm 0.1) \times 10^5$ M^{-1} s^{-1} and a k_{-1} of 16.6 ± 0.3 s^{-1} were calculated for the first binding step.[24] These values were then used to estimate an association constant, K_a, of $(1.6 \pm 0.1) \times 10^4$ M^{-1}. The same global kinetic analysis gave $k_2 = (4.1 \pm 0.5) \times 10^3$ M^{-1} s^{-1} and $k_{-2} = (3.9 \pm 0.6)$ s^{-1} for the second step. These latter values, while not well-determined, allowed an equilibrium constant of ca. 1×10^3 M^{-1} to be estimated for the second step. This value is an order of magnitude smaller than the K_a for the first event.

The data were also analyzed by conventional methods, wherein k_{obs} was plotted as a function of the guest concentration. This gave concordant values for the on and off rates for the first step as shown in Figure 4 and in Table 1 (the raw data are given in Figures S4−S7). Unlike acetate, the slower kinetics of interaction between **C8**·2HCl and $TBAH_2PO_4$ allowed for analysis of the dynamics over a range of temperatures. Figure 4 shows the results of such an analysis carried out at 243, 253, and 273 K.

To check the mechanistic assumptions on which the kinetic analysis was based, a steady-state titration was performed at 253 K in CH_3CN (cf., Figure 5a). This study was carried out under conditions identical to those used for the kinetic analysis, that is, the same temperature, concentration of **C8**·2HCl, and solvent. This congruity allowed us to compare with confidence the two sets of association constants obtained from these disparate procedures. With the exception of several initial points ascribed to the formation of a 1:2 (phosphate-to-**C8**) complex, a binding isotherm in agreement with the kinetic results was obtained when the concentration of the guest was plotted versus

(20) Iverson, B. L.; Shreder, K.; Král, V.; Sansom, P.; Lynch, V.; Sessler, J. L. *J. Am. Chem. Soc.* **1996**, *118*, 1608–16.
(21) Král, V.; Furuta, H.; Shreder, K.; Lynch, V.; Sessler, J. L. *J. Am. Chem. Soc.* **1996**, *118*, 1595–1607.
(22) The crystal structure of **C8** with a singly charged tetrahedral oxyanion (cf., Figure S3) revealed a 2:1 complex with the two anions held above and below the plane of the relatively flat macrocycle.
(23) Note that all the spectra obtained by stopped-flow measurements were taken as difference spectra in which the final spectrum was subtracted; recovery of the bleaching absorption at 400 nm in Figure 2b corresponds to the formation of the 1:2 complex.
(24) Johnson, K. A.; Simpson, Z. B.; Blom, T. *Anal. Biochem.* **2009**, *387*, 20–29.

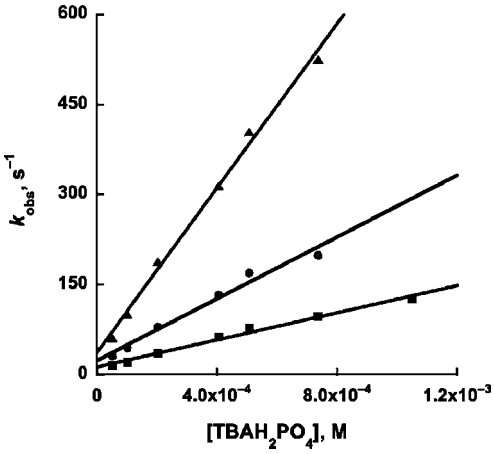

Figure 4. Plots of the pseudo-first-order rate constant versus the concentration of guest for the stopped-flow data involving **C8**·2HCl and $TBAH_2PO_4$ at 243 (■), 253 (●), and 273 (▲) K, wherein the concentration of the guest is in excess relative to the host. In this case, k_1 or k_{on} is given by the slope of the line, and k_{-1} or k_{off} is given by the *y*-intercept. These values are summarized in Table 1.

Table 1. Summary of the Calculated k_1 (k_{on}) and k_{-1} (k_{off}) and the Kinetically Derived Association Constants (K_a) for **C8**·2HCl and $H_2PO_4^-$

T, K	k_1, M^{-1} s^{-1a}	k_{-1}, s^{-1a}	K_a, M^{-1}	k_1, M^{-1} s^{-1}	k_{-1}, s^{-1b}	K_a, M^{-1}
298	3.9×10^6	84	4.6×10^4			
273	6.8×10^5	37	1.8×10^4	6.5×10^5	27.3	2.4×10^4
253	2.6×10^5	23	1.1×10^4	2.6×10^5	13.3	1.9×10^4
243	1.2×10^5	10	0.9×10^4			

[a] Rate constants and K_a calculated by the conventional method shown in the graph above. [b] Rate constants and K_a calculated by global fitting analysis using the KinTek software.[18]

the change in absorbance for **C8**.[25] Shown in Figure 5b is the overlay of the expected binding isotherm based on a simulation using the full set of kinetic data seen in Figure 3 and that obtained from an independent steady state analysis. Gratifyingly, the resulting binding curves match well.

A comparison between the association constants for **C8** and $H_2PO_4^-$ obtained at various temperatures was carried out. On this basis, it was inferred that the kinetically derived K_a value decreases with decreasing temperature. This is indicative of an endothermic reaction, wherein there is a largely positive entropy contribution. This is common for ion-pairing events, wherein desolvation occurs to afford a largely positive entropy change.[26,27] On the other hand, the complex itself is highly unrestrained (e.g., not held in a particular configuration). Given the planar structure of **C8** and the 2+ charge, such an inference seems reasonable.

These data also allowed for van't Hoff analyses, from which ΔH and ΔS values of 4.4 kcal mol^{-1} and 36 cal K^{-1} mol^{-1}, respectively, were determined.[28] A similar decrease in K_a as a function of temperature was also seen for TBAOAc, where the

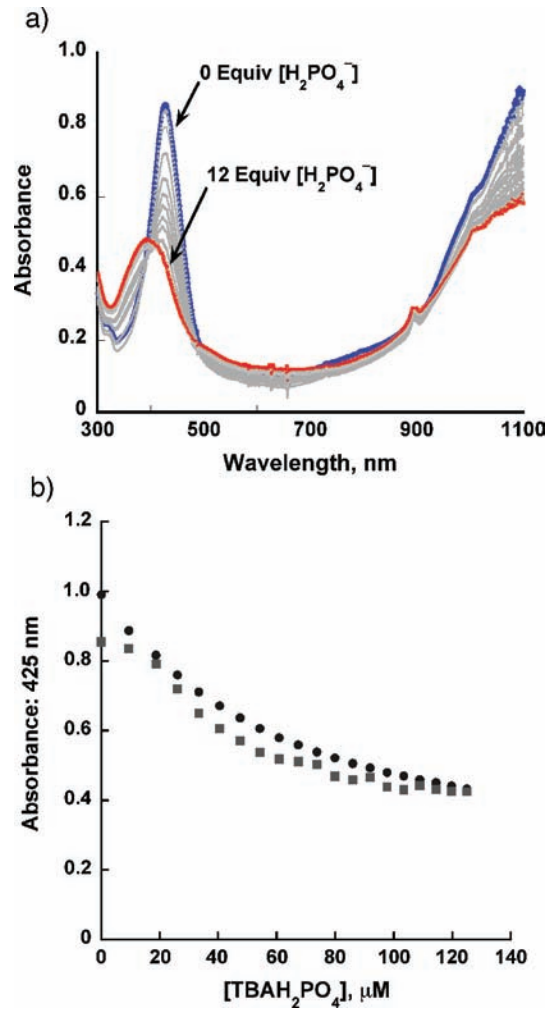

Figure 5. (a) Steady-state titration of **C8**·2HCl (11 μM) with increasing quantities of $TBAH_2PO_4$ in CH_3CN at 253 K. (b) Binding isotherm for the steady-state titration of **C8**·2HCl and $TBAH_2PO_4$ shown in part (a) (■) and the simulated binding isotherm based on a global fit to the kinetic data recorded at 253 K (●).

Table 2. Kinetic and Thermodynamic Parameters for the Binding of Indicated Guest in CH_3CN[a]

	AcO^-	$H_2PO_4^-$
ΔH (kcal mol^{-1})[b]	2.8	4.4
ΔS (cal K^{-1} mol^{-1})[b]	33.7	36
ΔG (kcal mol^{-1})[c]	−7.2	−6.3
$\Delta H_{ass}^{\ddagger}$ (kcal mol^{-1})[d]		8.3
$\Delta S_{ass}^{\ddagger}$ (cal K^{-1} mol^{-1})[d,e]		−3.0
$\Delta G_{ass}^{\ddagger}$ (kcal mol^{-1})[f]		9.2
$\Delta H_{diss}^{\ddagger}$ (kcal mol^{-1})[d]		4.6
$\Delta S_{diss}^{\ddagger}$ (cal K^{-1} mol^{-1})[d]		−34
$\Delta G_{diss}^{\ddagger}$ (kcal mol^{-1})[f]		14.7
ΔH ($\Delta H_{ass}^{\ddagger} - \Delta H_{diss}^{\ddagger}$) (kcal mol^{-1})		3.7
ΔS ($\Delta S_{ass}^{\ddagger} - \Delta S_{diss}^{\ddagger}$) (cal K^{-1} mol^{-1})		31
ΔG ($\Delta G_{ass}^{\ddagger} - \Delta G_{diss}^{\ddagger}$) (kcal mol^{-1})		−5.5

[a] Error for the listed values is estimated to be ≤10% unless otherwise noted. [b] Calculated from van't Hoff analysis shown in Figure 6. [c] Calculated using the Gibbs−Helmholtz equation $\Delta G = \Delta H - T\Delta S$ at 298 K. [d] Calculated from Eyring analysis shown in Figure 7. [e] Estimated error: 33%. [f] Calculated using the Gibbs−Helmholtz equation $\Delta G^{\ddagger} = \Delta H^{\ddagger} - T\Delta S^{\ddagger}$ at 298 K.

van't Hoff plot yielded a ΔH value of 2.8 kcal mol^{-1} and a ΔS value of 33.7 cal K^{-1} mol^{-1} (Figure 6b, Table 2).

Finally, the activation parameters for both the association and the dissociation processes were determined from Eyring plots

(25) For similar analyses, see: (a) Choi, K.; Hamilton, A. D. *J. Am. Chem. Soc.* **2003**, *125*, 10241–10249. (b) Hossain, M. A.; Llinares, J. M.; Powell, D.; Bowman-James, K. *Inorg. Chem.* **2001**, *40*, 2936–2937. (c) Kubik, S.; Goddard, R.; Kirchner, R.; Nolting, D.; Seidel, J. R. *Angew. Chem., Int. Ed.* **2001**, *40*, 2648–2651.
(26) Valik, M.; Král, V.; Herdtweck, E.; Schmidtchen, F. P. *New J. Chem.* **2007**, *31*, 703–710.
(27) Jadhav, V. D.; Herdtweck, E.; Schmidtchen, F. P. *Chem.-Eur. J.* **2008**, *14*, 6098–6107.
(28) Anslyn, E. V.; Dougherty, D. A. *Modern Physical Organic Chemistry*; University Science Books: Sausalito, CA, 2006.

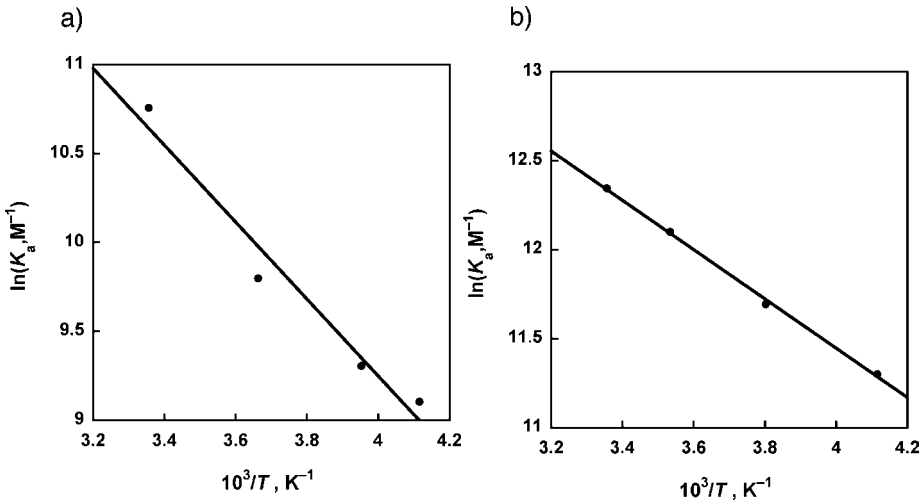

Figure 6. Van't Hoff analysis for **C8** with (a) $H_2PO_4^-$ and (b) AcO^-; here, ln K_a is plotted as a function of $1/T$. This is based on the equation ln $K_a = (\Delta S/R) - (\Delta H/RT)$, which yields $\Delta H/R$ as the slope and $\Delta S/R$ as the y-intercept.

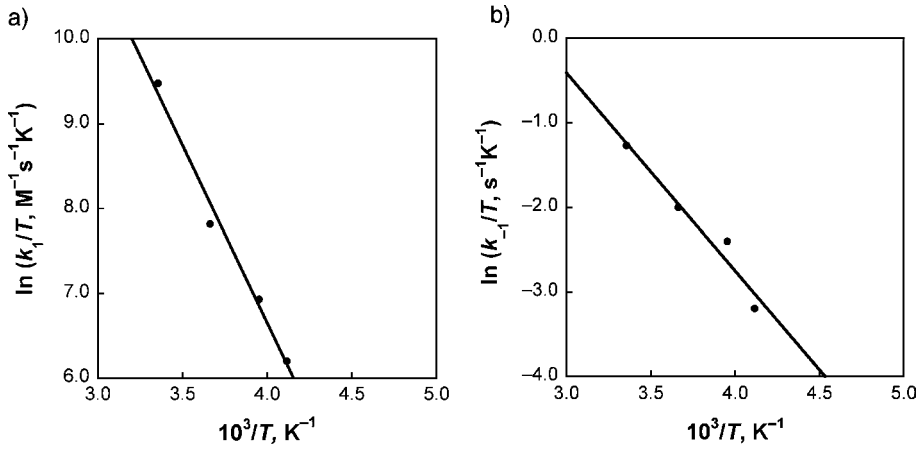

Figure 7. Eyring plots constructed using the (a) on rates and (b) off rates from Table 1. This plot is based on the following equation: $\ln(k/T) = [\ln(k_B/h) + \Delta S^{\ddagger}/R] - \Delta H^{\ddagger}/(RT)$.

(Figure 7). Here, the on and off rates were analyzed separately as a function of temperature and fit to the following equation: $\ln(k/T) = [\ln(k_B/h) + \Delta S^{\ddagger}/R] - \Delta H^{\ddagger}/(RT)$.[29] The resulting values are included in Table 2. In the case of dihydrogen phosphate, the activation enthalpy ($\Delta H_{ass}^{\ddagger}$) and entropy ($\Delta S_{ass}^{\ddagger}$) for the association of dihydrogen phosphate with **C8** were determined to be $\Delta H_{ass}^{\ddagger} = 8.3$ kcal mol^{-1} and $\Delta S_{ass}^{\ddagger} = -3.0$ cal K^{-1} mol^{-1}, respectively (cf., Figure 6a). The $\Delta H^{\ddagger}$ and $\Delta S^{\ddagger}$ values for the dissociation were also determined: $\Delta H_{diss}^{\ddagger} = 4.6$ kcal mol^{-1} and $\Delta S_{diss}^{\ddagger} = -34$ cal K^{-1} mol^{-1}, respectively (cf., Figure 6b). These values allowed a "check" for $\Delta H = \Delta H_{ass}^{\ddagger} - \Delta H_{diss}^{\ddagger} = 3.7$ kcal mol^{-1} and $\Delta S = \Delta S_{ass}^{\ddagger} - \Delta S_{diss}^{\ddagger} = 31$ cal K^{-1} mol^{-1} to be carried out. The standard free energy, ΔG, was then calculated to be -5.5 kcal mol^{-1} at 298 K. In accord with expectations, these kinetically derived values were found to agree well within experimental error with those determined by the van't Hoff analysis described above (i.e., $\Delta H = 4.4$ kcal mol^{-1} and $\Delta S = 36$ cal K^{-1} mol^{-1}, and at 298 K, $\Delta G = -6.3$ kcal mol^{-1}).

Conclusion

The present kinetic studies provide support for the notion that observable differences can underlie the binding of different guests. For instance, even under conditions designed to slow the reaction (low temperature; dilute conditions), the interaction between **C8** and acetate achieves equilibrium in about 10 ms in CH_3CN to give a 1:1 complex. Furthermore, no evidence of additional complexation is seen under any of the tested conditions using this particular anion. On the other hand, in the case of dihydrogen phosphate, a 2:1 complex is formed with kinetics that are much slower than those associated with the formation of the initial, dominant 1:1 complex. On the basis of the notable differences seen for these two test anions, we propose that kinetic analyses will have an important role to play in the advanced characterization of new anion binding agents.

Acknowledgment. This work was supported by the National Institutes of Health (grant GM 58907 to J.L.S.), the Robert A. Welch Foundation (grant F-1018 to J.L.S.), and a Grant-in-Aid (Nos. 21750146 and 20108010) and a Global COE program, "the Global Education and Research Center for Bio-Environmental Chemistry", from the Ministry of Education, Culture, Sports, Science and Technology, Japan to K.O. and S.F. Support to J.L.S. and S.F. under the Korean WCU program is also acknowledged (grants R32-20080-000-10217-0 and R31-2008-000-10010-0, respectively).

Supporting Information Available: Experimental procedures and Figures S1−S10. This material is available free of charge via the Internet at http://pubs.acs.org.

JA107471X

(29) Connors, K. A. *Chemical Kinetics*; VCH Publishers: New York, 1990.